Research article

N. Asger Mortensen*, P. A. D. Gonçalves, Fedor A. Shuklin, Joel D. Cox, Christos Tserkezis, Masakazu Ichikawa and Christian Wolff

Surface-response functions obtained from equilibrium electron-density profiles

https://doi.org/10.1515/nanoph-2021-0084
Received March 1, 2021; accepted April 19, 2021;
published online May 7, 2021

Abstract: Surface-response functions are one of the most promising routes for bridging the gap between fully quantum-mechanical calculations and phenomenological models in quantum nanoplasmonics. Among all currently available recipes for obtaining such response functions, the use of *ab initio* methods remains one of the most conspicuous trends, wherein the surface-response functions are retrieved via the metal's non-equilibrium response to an external time-dependent perturbation. Here, we present a complementary approach to approximate one of the most appealing surface-response functions, namely the Feibelman d-parameters, yield a finite contribution even when they are calculated solely with the equilibrium properties of the metal, described under the local-response approximation (LRA) but with a spatially varying equilibrium electron density, as input. Using model calculations that mimic both spill-in and spill-out of the equilibrium electron density, we show that the obtained d-parameters are in qualitative agreement with more elaborate, but also more computationally demanding, *ab initio* methods. The analytical work presented here illustrates how microscopic surface-response functions can emerge out of entirely local electrodynamic considerations.

Keywords: electrodynamics; Landau damping; nonlocal response; quantum plasmonics; surface-response formalism.

1 Introduction

The plasmonic response of metallic nanostructures is commonly explored within the framework of classical electrodynamics [1], typically describing the free electrons of metals classically within the Drude-like local-response approximation (LRA) [2]. The classical LRA prescription thus treats a metal as a homogeneous gas of noninteracting electrons confined by a hard wall at the metal's surface. In this fashion, any aspects of nonlocal (i.e., q-dependent) response [3–5] are commonly neglected both in the bulk of the metal (e.g., finite compressibility of the Fermi gas) and at its surface (e.g., Friedel oscillations and electronic spill-out associated with a finite work function).

Despite neglecting quantum-mechanical effects, the LRA has constituted a critical theoretical framework in the overall development of plasmonics [2, 6, 7]. More recently, the importance of quantum phenomena has been pursued via classical accounts, including smooth equilibrium electron-density profiles [8–10], semiclassical hydrodynamic models [11–13], and *ab initio* studies [14, 15]. The former approaches can be criticized for only dealing with some quantum aspects semiclassically, while the latter are typically restricted by their complexity and by their practical applicability to small plasmonic systems [16–20]. In this context, surface-response functions aim to capture the dominant quantum phenomena and microscopic aspects of the surface, while still allowing for a (semi)classical treatment of the light–matter interactions in the bulk of the metal. As such, there has recently been a renewed interest in electrodynamic surface-response functions [21–23]

***Corresponding author**: **N. Asger Mortensen**, Center for Nano Optics, University of Southern Denmark, Campusvej 55, DK-5230 Odense M, Denmark; Danish Institute for Advanced Study, University of Southern Denmark, Campusvej 55, DK-5230 Odense M, Denmark; and Center for Nanostructured Graphene, Technical University of Denmark, DK-2800 Kongens Lyngby, Denmark,
E-mail: asger@mailaps.org. https://orcid.org/0000-0001-7936-6264
P. A. D. Gonçalves, **Fedor A. Shuklin**, **Christos Tserkezis and Christian Wolff**, Center for Nano Optics, University of Southern Denmark, Campusvej 55, DK-5230 Odense M, Denmark, E-mail: pa@mci.sdu.dk (P. A. D. Goncalves), fesh@mci.sdu.dk (F. A. Shuklin), ct@mci.sdu.dk (C. Tserkezis), cwo@mci.sdu.dk (C. Wolff). https://orcid.org/0000-0001-8518-3886 (P. A. D. Gonçalves)
Joel D. Cox, Center for Nano Optics, University of Southern Denmark, Campusvej 55, DK-5230 Odense M, Denmark; and Danish Institute for Advanced Study, University of Southern Denmark, Campusvej 55, DK-5230 Odense M, Denmark, E-mail: cox@mci.sdu.dk
Masakazu Ichikawa, Department of Applied Physics, Graduate School of Engineering, The University of Tokyo, Bunkyo-ku, Tokyo 113-8656, Japan, E-mail: ichikawa@ap.t.u-tokyo.ac.jp

in the context of plasmon-enhanced light–matter interactions [24–27] and quantum plasmonics [28–30], emphasizing their importance in plasmon–emitter interactions in nanoscale environments [26, 27], plasmon-enhanced interactions with two-dimensional (2D) materials [27, 31], and in revealing the detailed spectral properties of plasmon resonances themselves [18, 26, 32–36].

Traditionally, surface-response functions have been obtained through first-principle calculations of the electrodynamics of metal surfaces subjected to time-varying electric fields [37], e.g., by employing time-dependent density-functional theory (TDDFT) [14], while they can, in some cases, also be analytically evaluated, e.g., from semiclassical hydrodynamic models [34, 38–40]. In all cases, the common strategy has been to first evaluate the nonequilibrium response to obtain the induced charge density, $\rho_{\text{ind}}(\omega; \mathbf{r}_{\hat{\mathbf{n}}})$, and extract from it the surface-response function(s), e.g., the Feibelman $d_\perp$-parameter (corresponding to the centroid of induced charge density [21]). Here, we explicitly show that even when using a local-response approach along with the equilibrium electron density-profile alone as input, there is a finite contribution to the metallic surface-response functions provided that the (equilibrium) electron density varies smoothly from its bulk value deep inside the metal to zero near the metal's surface [41–43] (as opposed to terminating abruptly at it). Such an approach, despite its simplicity and inherent limitations, could nevertheless facilitate new physical insights into the electrodynamic fingerprints associated with quantum spill-out/spill-in, without resorting to computationally demanding *ab initio* methods. We should, however, emphasize that the approach presented below ignores the finite compressibility of the electron gas, already captured by semiclassical hydrodynamic models [5], as well as more complicated many-body effects and correlations that time-dependent *ab initio* methods seek to capture, while naturally still resorting to approximations [14].

2 Results

We consider a metallic nanostructure where $n_0(\mathbf{r})$ is the equilibrium electron density (see Figure 1a), which is spatially inhomogeneous in the vicinity of the metal's surface, possibly including, e.g., quantum spill-out and/or Friedel oscillations [44] due to a finite work function [45]. In the presence of time-harmonic electromagnetic fields, the electrodynamics of the system is governed by the integro-differential wave equation

$$\nabla \times \nabla \times \mathbf{E}(\mathbf{r}) = \frac{\omega^2}{c^2} \int \mathrm{d}\mathbf{r}'\, \varepsilon(\mathbf{r}, \mathbf{r}')\mathbf{E}(\mathbf{r}'), \tag{1}$$

where ω is the angular frequency, c is the speed of light in vacuum, and $\varepsilon(\mathbf{r}, \mathbf{r}')$ is the nonlocal linear-response function, i.e., the (nonlocal) dielectric function of the quantum electron gas (here assumed to be isotropic, for the sake of simplicity). The microscopic and analytical understanding of $\varepsilon(\mathbf{r}, \mathbf{r}')$ is in general limited to bulk considerations within the random-phase approximation (RPA) or the hydrodynamic model (HDM) [4, 5, 27, 41, 46, 47].

2.1 Local-response approximation

In order to proceed with the nonlocal, integro-differential wave equation (1), it is common to invoke further approximations — in the context of plasmonics, the prevailing one being the LRA, epitomized by

$$\varepsilon(\mathbf{r}, \mathbf{r}') \approx \varepsilon_{\text{LRA}}(\mathbf{r})\delta(\mathbf{r} - \mathbf{r}'). \tag{2a}$$

Here, the inherently finite-range associated with the nonlocal response of the electron gas is neglected in favor of a zero-range, *local* response (mathematically represented by the Dirac delta function in the previous expression). Physically, this is equivalent to neglecting spatial dispersion represented by a finite wave vector dependence of the dielectric function [4, 5, 27], and thus ignoring, for instance, the finite dynamic compressibility of the electron gas [4, 5]. In spite of this — and as we show in what follows — some quantum aspects associated with an inhomogeneous electron gas (Figure 1a), like electronic spill-out, can still be incorporated to some extent in the LRA. In particular, the LRA reduces the nonlocal wave equation (1) to the familiar local-response one:

$$\nabla \times \nabla \times \mathbf{E}(\mathbf{r}) = \frac{\omega^2}{c^2}\varepsilon_{\text{LRA}}(\mathbf{r})\mathbf{E}(\mathbf{r}), \tag{2b}$$

which is conceptually simpler and computationally more tractable [48].

2.2 Piecewise-constant approximation (PCA)

Inspired by the long-established traditions in the electrodynamics of composite dielectric problems [49], it is common in plasmonics [2] to invoke yet another approximation: the step-like, abrupt surface termination of the metal, thereby neglecting any microscopic inhomogeneities in the vicinity of the surface [herein defined by $z = 0$, without loss of generality, with the metal and the dielectric each occupying the $z < 0$ and $z > 0$ half-spaces, respectively (Figure 1a)]. Under this approximation, $\varepsilon_{\text{LRA}}(z) \to \varepsilon_{\text{PCA}}(z)$, with

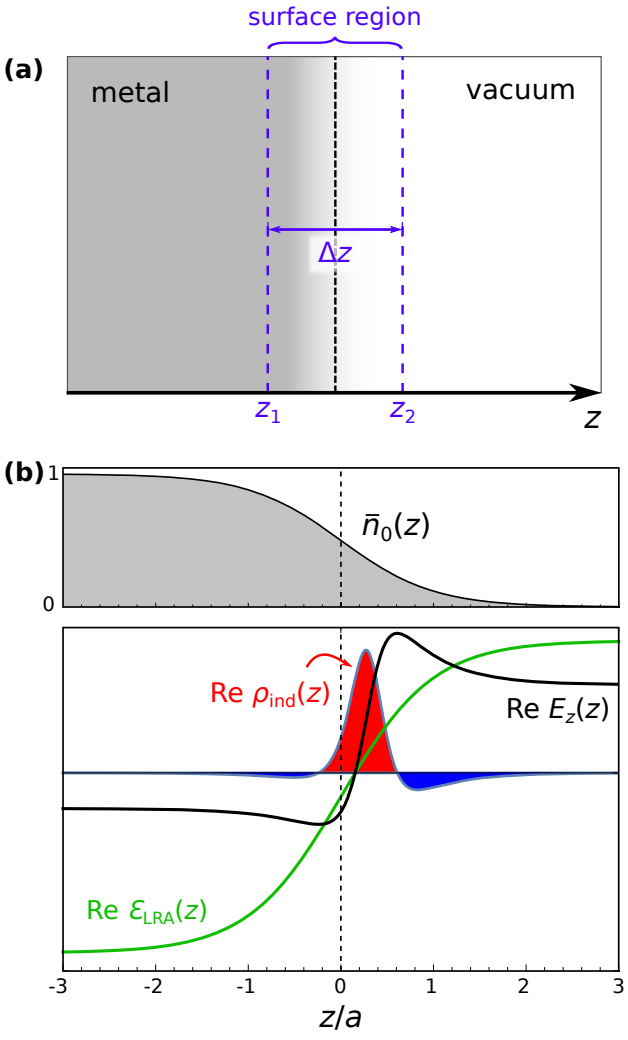

Figure 1: Schematic representation of the microscopic features of a metal–vacuum interface. (a) Metal–vacuum interface, indicating the surface region where the electron density varies from its asymptotic, bulk values $\varepsilon_{\rm m} \equiv \varepsilon_{\rm LRA}(z < z_1)$ and $\varepsilon_{\rm d} \equiv \varepsilon_{\rm LRA}(z > z_2) = 1$ (where $|z_{1,2}| \gg 0$). (b) Top: schematic of the (normalized) equilibrium electron-density profile $\bar{n}_0(z)$ characterized by a smearing length a in the vicinity of the surface (here defined by the $z = 0$ plane). Bottom: Real part of the system's dielectric function Re $\varepsilon_{\rm LRA}(z)$ [Eq. (8)] associated with $\bar{n}_0(z) = [1 - \tanh(z/a)]/2$, along with the ensuing Re $E_z(z)$ and Re $\rho_{\rm ind}(z)$ [note that $\rho_{\rm ind} \propto \partial_z \varepsilon_{\rm LRA}^{-1}$ in the long-wavelength regime]. All quantities are in arbitrary units. Parameters: $\omega = \omega_{\rm p}/\sqrt{3}$, and for visualization purposes a Drude-type bulk damping of $\gamma/\omega_{\rm p} = 0.3$.

$$\varepsilon_{\rm PCA}(z) \equiv \varepsilon_{\rm LRA}(-\infty)\Theta(-z) + \varepsilon_{\rm LRA}(\infty)\Theta(z) \tag{3a}$$

$$\equiv \varepsilon_{\rm m}\Theta(-z) + \varepsilon_{\rm d}\Theta(z), \tag{3b}$$

where Θ is the Heaviside step function, and the system's dielectric function is constructed from two interfacing piecewise-constant (bulk) local-response functions, $\varepsilon_{\rm m} \equiv \varepsilon_{\rm m}(\omega)$ and $\varepsilon_{\rm d} \equiv \varepsilon_{\rm d}(\omega)$ (and Eq. (2b) is then solved by invoking the classical pillbox arguments at the interface [1]). Here, $\varepsilon_{\rm m}$ is the Drude-like dielectric function of the free-electron gas [2, 11]

$$\varepsilon_{\rm m} = \varepsilon_+ - \frac{\omega_{\rm p}^2}{\omega^2 + {\rm i}\omega\gamma}, \tag{4}$$

with $\varepsilon_+ \equiv \varepsilon_+(\omega)$ allowing for the incorporation of the polarization due to the positive ionic background or for a heuristic account of interband transitions. It should be emphasized that the PCA has been tremendously successful in advancing the field of plasmonics, being sufficient to interpret the majority of experimentally observed phenomena [2]. What makes the PCA legitimate in most cases is the fact that the electron density is only non-uniform across an extremely small region in the vicinity of the metal surface, typically spanning only a few ångströms (i.e., on the order to the metal's bulk Fermi wavelength, $\lambda_{\rm F}$). In spite of this, such a "classical" PCA is currently being challenged by the recent developments in nanoscale plasmonics and plasmon-empowered light–matter interactions at nanometric scales [15, 25–27, 31, 35, 50].

2.3 Surface-response formalism

In the PCA, the induced charge is strictly a (singular) surface charge, i.e., $\rho_{\rm ind}(z) \propto \delta(z)$ [1, 21, 27], while in reality, the induced charge actually assumes a nonsingular density of a finite, surface-peaked nature (Figure 1b). In this context, the Feibelman d-parameters, $d_\perp \equiv d_\perp(\omega)$ and $d_\parallel \equiv d_\parallel(\omega)$, are dynamical surface-response functions that correspond to the first moment (i.e., the centroid) of the induced charge density and of the normal derivative of the tangential current density, given, respectively, by (ω-dependence implicit) [21]

$$d_\perp = \frac{\int_{-\infty}^{\infty} {\rm d}z\, z\, \rho_{\rm ind}(z)}{\int_{-\infty}^{\infty} {\rm d}z\, \rho_{\rm ind}(z)}, \quad d_\parallel = \frac{\int_{-\infty}^{\infty} {\rm d}z\, z\, \frac{\partial}{\partial z} J_x^{\rm ind}(z)}{\int_{-\infty}^{\infty} {\rm d}z\, \frac{\partial}{\partial z} J_x^{\rm ind}(z)}, \tag{5}$$

which are complex-valued surface-response functions, i.e., $d_\alpha(\omega) = d'_\alpha(\omega) + {\rm i}d''_\alpha(\omega)$ with $\alpha \in \{\perp, \parallel\}$. The general appeal of the d-parameters is that, once they are obtained, the system's optical response can be calculated by solving a d-parameter-modified electrodynamic problem, namely, the LRA wave Eq. (2b) together with the "classical" PCA [recall Eq. (3a)] but now subjected to the d-parameter-corrected, mesoscopic boundary conditions [26, 27, 33–35]. Computationally, this is clearly more attractive than having to solve the more complex integro-differential problem typified by Eq. (1), while at the same time such reformulation into a

quantum-informed "classical-equivalent" electrodynamic problem also paves the way for further analytical work [26, 27, 34]. Naturally, different mechanisms can be incorporated (together or separately) via the d-parameters, e.g., nonlocality, quantum spill-out/spill-in, Landau damping, etc. [21, 51]. In the following, we limit our consideration to the LRA contribution to the d-parameters emerging solely from a spatially varying dielectric function, i.e., $\varepsilon_{\mathrm{LRA}}(z)$.

Alternatively to Eq. (5), the d-parameters can also be written in terms of surface integrals associated with the difference between the actual, microscopic fields and the classical, "Fresnel" fields stemming from the PCA [21, 22, 52–58], specifically (see Supplementary Material):

$$d_{\perp} = -\frac{\varepsilon_{\mathrm{d}}}{\varepsilon_{\mathrm{m}} - \varepsilon_{\mathrm{d}}} \int_{-\infty}^{\infty} \mathrm{d}z \, \frac{E_z(z) - E_z^{\mathrm{PCA}}(z)}{E_z^{\mathrm{PCA}}(0^-)}, \tag{6a}$$

$$d_{\parallel} = \frac{1}{\varepsilon_{\mathrm{m}} - \varepsilon_{\mathrm{d}}} \int_{-\infty}^{\infty} \mathrm{d}z \, \frac{D_x(z) - D_x^{\mathrm{PCA}}(z)}{\varepsilon_0 E_x^{\mathrm{PCA}}(0^-)}, \tag{6b}$$

where $E_{x,z}^{\mathrm{PCA}}, D_x^{\mathrm{PCA}}$ are fields obtained within the classical, piecewise-constant approach. In the long-wavelength regime and to leading-order in $q|z_2 - z_1|$, the Feibelman d-parameters (6) associated with a local, but smoothly varying dielectric function $\varepsilon_{\mathrm{LRA}}(z)$ can be written as [55, 59–62] (see Supplementary Material)

$$d_{\perp} = \frac{1}{\epsilon_{\mathrm{m}}^{-1} - \epsilon_{\mathrm{d}}^{-1}} \int_{-\infty}^{\infty} \mathrm{d}z \, \left[\varepsilon_{\mathrm{LRA}}^{-1}(z) - \varepsilon_{\mathrm{PCA}}^{-1}(z)\right], \tag{7a}$$

$$d_{\parallel} = \frac{1}{\epsilon_{\mathrm{m}} - \epsilon_{\mathrm{d}}} \int_{-\infty}^{\infty} \mathrm{d}z \, \left[\varepsilon_{\mathrm{LRA}}(z) - \varepsilon_{\mathrm{PCA}}(z)\right]. \tag{7b}$$

Equations (7) unambiguously illustrate how $\varepsilon_{\mathrm{LRA}}(x) \neq \varepsilon_{\mathrm{PCA}}(x)$ contributes to a finite $d_{\perp}$ and $d_{\parallel}$. Naturally, in general, there will be further contributions to the d-parameters stemming from the nonlocal response of the electron gas (e.g., treated within the nonlocal RPA or the HDM); nevertheless, it is important to emphasize that there is a nonzero contribution to the surface-response already within the LRA once the PCA is relaxed. In the following, we shall illustrate this in more detail with an elementary model that elucidates the physics — within the constraints associated with the LRA — of both spill-out and spill-in of the metal's electron density. Despite its inherent simplicity, the strength of the simple model adopted below lies in its ability to render analytical results in closed form.

2.4 Metal surface with a smoothly varying electron density

As mentioned previously, a more realistic representation of a metal surface is to abandon the assumption of an infinitely sharp dielectric–metal interface and instead allow the metal's electron density to vary smoothly from its value deep inside the metal, $n_0^{\mathrm{bulk}} \equiv n_0(z \to -\infty)$, to zero well inside the vacuum (Figure 1). This can be modeled through a simple generalization [21, 38, 41–43, 63, 64] of Eq. (4), that is

$$\varepsilon_{\mathrm{LRA}}(z) = \varepsilon_{\infty}(z) - \frac{\omega_{\mathrm{p}}^2}{\omega^2 + \mathrm{i}\omega\gamma} \bar{n}_0(z), \quad \bar{n}_0(z) = \frac{n_0(z)}{n_0^{\mathrm{bulk}}}. \tag{8}$$

where $n_0(\mathbf{r}) \equiv n_0(z)$ is the spatial profile of the equilibrium electron density. Here, $\varepsilon_{\infty}(z)$ takes into account the variation from the background polarization, subjected to the requirement that deep inside the metal (dielectric) it converges to the polarization due to the jellium background of positive ions, $\varepsilon_{\infty}(z \to -\infty) = \varepsilon_{+}$ (to the dielectric's permittivity $\varepsilon_{\infty}(z \to +\infty) = \varepsilon_{\mathrm{d}}$). As a complementary perspective, this can also be interpreted as the common local response of the Drude kind, but with a spatially varying plasma frequency, $\omega_{\mathrm{p}}(z) \equiv \omega_{\mathrm{p}}\sqrt{\bar{n}_0(z)}$. In passing, we note that Eq. (8) has been used widely over the years, including Refs. [8, 9, 65–70], while smoothly varying profiles have also been considered in model discussions of local-field corrections [71]. Finally, we note how the PCA mathematically emerges upon replacing $\bar{n}_0(z)$ by a Heaviside function in Eq. (8), i.e., $\bar{n}_0(z) \to \Theta(-z)$, corresponding to the classical, step-like termination of the equilibrium electron density.

2.5 Transition from spill-in to spill-out

To illustrate the transition from spill-in to spill-out, we consider a model electron-density profile of the form [62]

$$\bar{n}_0(z) = \tanh^2\left(\frac{z - z_0}{a}\right) \Theta(z_0 - z), \tag{9}$$

which is smooth and has the desired properties $\lim_{z\to-\infty}\bar{n}_0(z) = 1$ and $\lim_{z\to+\infty}\bar{n}_0(z) = 0$ [in fact, the latter can be made more stringent, e.g., $\lim_{z\to z_0}\bar{n}_0(z) = 0$]. The value z_0 indicates the position where the metal's electron density vanishes, whereas the quantity a charactokerizes the steepness of the spatial profile of the (normalized) equilibrium electron density [with $\lim_{a\to 0}\bar{n}_0(z) = \Theta(z_0 - z)$]. The quantity z_0, in particular, governs whether the induced electron density spills inwards or outwards. For bulk electron densities of typical plasmonic metals, both a and z_0 amount to a few ångströms, and the model qualitatively

captures the main results of self-consistent jellium considerations [45], while more refined models are needed to also represent finer details, e.g., Friedel oscillations [44, 72].

Further, we assume that the transition from the jellium background (i.e., the metal's positively charged ions) to the dielectric remains infinitely sharp because these only contain tightly bound electrons which are thus essentially immobile[1] when compared with the conductive free-electrons; hence, in the following we take

$$\varepsilon_\infty(z) = \varepsilon_+\Theta(-z) + \varepsilon_d\Theta(z), \tag{10}$$

where we have assumed, without loss of generality, that the edge of jellium background is located at $z_b = 0$. In passing, we note that if we enforce charge neutrality, then a and z_0 are not independent, and $d_\parallel = 0$ (for the electron-density profile considered here (9), this would set $z_0 = a$). In spite of this, in what follows we assume that a and z_0 can be varied independently, as this may facilitate the treatment of charged metal surfaces (i.e., arising from either surface roughness, molecular adsorption, or the presence of Shockley surface states).

Going beyond jellium models, we note that care should be taken when turning to atomistic representations of the surface, where the choice of origin is reflected in the corresponding surface-response functions [36] (although the overall quantum surface-response is unchanged provided that both $d_\perp$ and $d_\parallel$ are considered).

2.6 Simple jellium next to vacuum

For clarity purposes, we first ignore background polarization effects or interband transitions and consider a simple jellium–vacuum interface, so that $\varepsilon_+ = \varepsilon_d = 1$. In this case, the integrals in Eqs. (7) yield

$$d_\perp(\Omega) = z_0 - a\,\tilde{\Omega}\,\mathrm{arctanh}\left(\tilde{\Omega}^{-1}\right), \tag{11a}$$

$$d_\parallel(\Omega) = z_0 - a. \tag{11b}$$

where $\Omega = \omega/\omega_p$ and $\tilde{\Omega} = \sqrt{\Omega(\Omega + i\Gamma)}$, with $\Gamma = \gamma/\omega_p$. As we shall see, the frequency-independent result for $d_\parallel$ is a particular consequence of having assumed $\varepsilon_+ = \varepsilon_d$. In the absence of bulk damping ($\Gamma \to 0^+$), Eq. (11a) can be written as [62]

$$d_\perp(\Omega) = z_0 + a\,\frac{\Omega}{2}\left[\ln\left|\frac{\Omega-1}{\Omega+1}\right| + i\pi\Theta(1-\Omega)\right], \tag{12}$$

with the low-frequency behavior of $d_\perp$ given by

$$\mathrm{Re}\,d_\perp(\Omega \ll 1) \simeq z_0, \tag{13a}$$

$$\mathrm{Im}\,d_\perp(\Omega \ll 1) \simeq a\,\frac{\pi}{2}\Omega. \tag{13b}$$

Notice that, even in the absence of *bulk* damping, there is a nonzero contribution of *surface-assisted* damping embodied through $\mathrm{Im}\,d_\perp \neq 0$ [see Eq. (13b)]. More fundamentally, this is a consequence of Kramers–Kronig relations (wherein a dispersive $\mathrm{Re}\,d_\perp$ renders $\mathrm{Im}\,d_\perp \neq 0$) [73]. Moreover, we emphasize that the asymptotic limits (13) are in agreement with results emerging from sum-rule considerations [74, 75]. Interestingly, in the above result, z_0 resembles the so-called static image-plane position that emerges from a self-consistent solution of the jellium perturbed by a static field [74–76], being a quantity of interest in surface science at large (a particular example being that of the van der Waals interaction of an atom near a metallic surface [52, 74]). Recently, acoustic graphene plasmons have been proposed as a mean to probe the quantum surface-response of metals [31] by placing a graphene sheet only a few nanometers away from a metal surface [77, 78]. In particular, the static surface-response, $d_\perp(0)$ [which, within our simple treatment, amounts to z_0; see Eq. (13a)], dependence could be experimentally probed in this way [31].

The results [Eqs. (11)–(12)] for a simple jellium surface next to vacuum are presented in Figure 2, showing how $\mathrm{Re}\,d_\perp$ is always negative for $z_0 = 0$ (Figure 2a; black curve). Increasing z_0/a brings the low-frequency part of $\mathrm{Re}\,d_\perp$ to positive values (Figure 2a; light-red and red curves), potentially extending into the frequency regime $\omega_p/\sqrt{3} \le \omega < \omega_p$ supporting semiclassical (specifically, within the HDM) localized surface plasmon (LSP) resonances in metal nanoparticles [79]. Consistent with causality and Kramers–Kronig relations, the dispersiveness of $\mathrm{Re}\,d_\perp$ is accompanied by a finite $\mathrm{Im}\,d_\perp$ (green, Figure 2a; orange, Figure 2b) [73–75].

2.7 Dipolar resonance of a metallic nanosphere

To illustrate how the surface-response functions $d_\perp$ and $d_\parallel$ jointly influence the optical response of a metallic nanostructure (Figure 2b), we consider the prototypical case of a spherical nanoparticle of radius R; for simplicity, we take $\varepsilon_+ = 1$ and assume that the nanosphere is in vacuum ($\varepsilon_d = 1$). Within the classical quasistatic LRA description the spectrum of LSP resonances is dominated by a size-independent dipole resonance at the frequency

1 We note, however, that this might not be the case for polar materials near optical phonon frequencies.

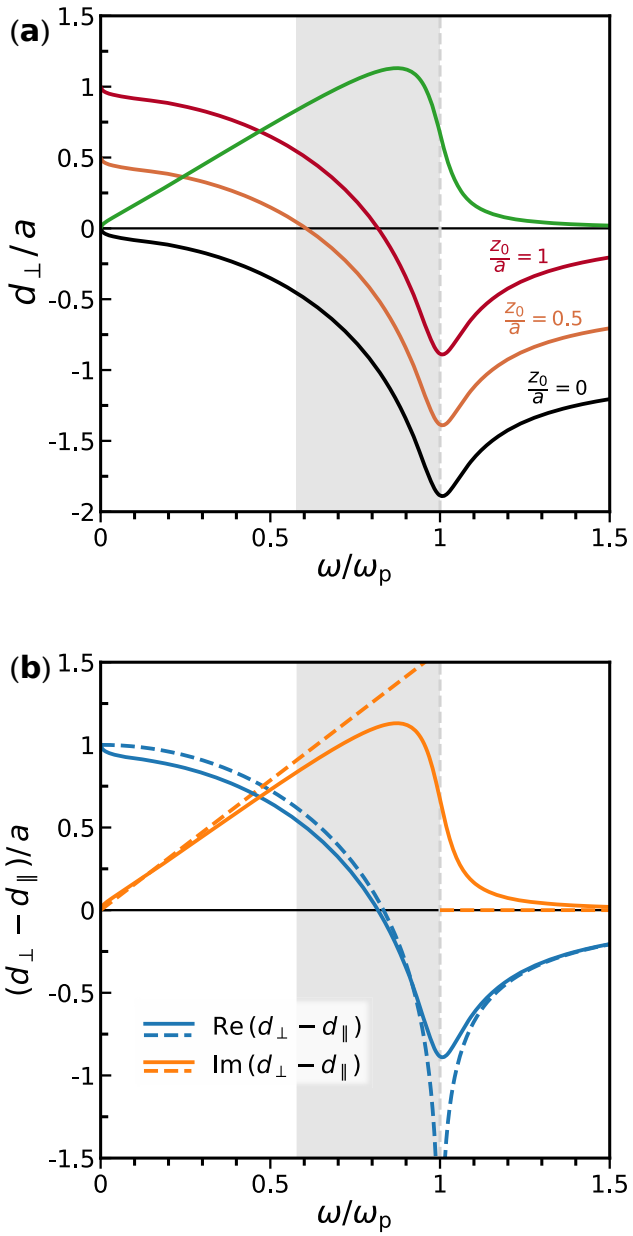

Figure 2: Feibelman d-parameters in the LRA for a jellium–vacuum interface ($\varepsilon_+ = \varepsilon_d = 1$) characterized by a smooth electron-density profile. (a) Real, Re $d_\perp$ (black, light-red, red), and imaginary part, Im $d_\perp$ (green) [Eq. (11a)] of the d-parameters for the electron-density profile described in Eq. (9) with varying z_0/a (whose effect is a simple vertical shift of the Re $d_\perp$ curve); we assume a Drude bulk damping of $\Gamma = \gamma/\omega_p = 0.1$. (b) Effective surface-response function $d_{\mathrm{eff}} \equiv d_\perp - d_\parallel$ [from Eq. (11)]. The dashed curves depict the result in the lossless case [62] [using Eqs. (11b) and (12)]. The grey-shaded region indicates the frequency window supporting semiclassical localized plasmon resonances in metallic nanoparticles.

$\omega = \omega_p/\sqrt{3}$ [2, 79, 80]. Accounting for nonclassical surface effects in a generalized Clausius–Mossotti relation, the pole associated with the dipolar LSP resonance is, to leading-order in $d_{\perp,\parallel}/R$, given by [26, 27, 34]

$$0 = \varepsilon_m + 2 - (\varepsilon_m - 1)\,\frac{2\,(d_\perp - d_\parallel)}{R}, \tag{14}$$

which illustrates how the smearing of the jellium near the surface of the particle causes nonclassical a/R size-dependent redshifts relative to the classical dipole resonance frequency (Figure 2b). Crucially, in this case, i.e., with $\varepsilon_+ = \varepsilon_d = 1$, the "effective" surface-response function $d_{\mathrm{eff}} \equiv d_\perp - d_\parallel$ [22, 27, 34] has a "universal" behavior, namely, it is (i) independent of z_0, and (ii) proportional to the smearing of the spatially varying electron-density profile, characterized by the length a. Thus, interestingly, these behaviors indicate that, independently of z_0, the smearing itself contributes to a net nonclassical redshift ($\mathrm{Re}\,d_{\mathrm{eff}} > 0$; spill-out) of the dipolar LSP resonance position of a jellium nanosphere in vacuum [81].

In the following, we simultaneously relax the assumptions of $\varepsilon_d = 1$ and of $\varepsilon_+ = 1$. Allowing the latter quantity to be larger than unity is commonly used to heuristically incorporate semiclassical accounts of background polarization effects or contributions arising from interband transitions in noble metals [2, 11].

2.8 Background and dielectric screening contributions

Turning to the general case of arbitrary ε_+ and ε_d, the effort required to perform the integrals (7) becomes somewhat more elaborate, but nevertheless these integrals can still be evaluated analytically, reading (assuming $z_0 \geq 0$)

$$\frac{d_\perp}{a} = C_\perp \left\{ \frac{1-\tilde{\Omega}^2\varepsilon_+}{1-\tilde{\Omega}^2\varepsilon_d}\frac{z_0}{a} - \frac{\varepsilon_d}{\sqrt{\varepsilon_+}}\tilde{\Omega}\left[\mathrm{arctanh}\left(\frac{\tilde{\Omega}^{-1}}{\sqrt{\varepsilon_+}}\right) - \mathrm{arctanh}\left(\frac{\tilde{\Omega}^{-1}}{\sqrt{\varepsilon_+}}\,\tanh\left(\frac{z_0}{a}\right)\right)\right] - \frac{\varepsilon_m\sqrt{\varepsilon_d}}{\varepsilon_m + (\varepsilon_d - \varepsilon_+)}\tilde{\Omega}\,\mathrm{arctanh}\left(\frac{\tilde{\Omega}^{-1}}{\sqrt{\varepsilon_d}}\,\tanh\left(\frac{z_0}{a}\right)\right)\right\}, \tag{15a}$$

$$\frac{d_\parallel}{a} = C_\parallel\,\frac{z_0 - a}{a}, \tag{15b}$$

where $C_\perp \equiv \left[1 + (\varepsilon_d - \varepsilon_+)\tilde{\Omega}^2\right]^{-1}$ and $C_\parallel \equiv (\varepsilon_m - \varepsilon_+)(\varepsilon_m - \varepsilon_d)$ are both being resonantly enhanced in the vicinity of $\omega = \omega_p/\sqrt{\varepsilon_+ - \varepsilon_d}$; this Bennett-type resonance [82, 83] should not be confused with the common surface

plasmon resonance occurring at $\omega = \omega_p/\sqrt{\varepsilon_+ + \varepsilon_d}$. Moreover, contrasting with the previous case (where $\varepsilon_+ = \varepsilon_d = 1$), now *both* $d_\perp$ and $d_\parallel$ are dispersive (i.e., exhibit frequency dependence). Finally, we note that these factors reduce to $C_\perp = C_\parallel = 1$ in the $\varepsilon_+ = \varepsilon_d$ case. Additionally, in this particular case, $d_\perp$ and $d_\parallel$ are given by Eq. (11) upon replacing $\tilde{\Omega}^{-1} \to \tilde{\Omega}^{-1}/\sqrt{\varepsilon}$, where $\varepsilon \equiv \varepsilon_+ = \varepsilon_d$.

Returning to the discussion surrounding Eq. (14), we note that, in addition to the nonclassical a/R-dependent redshift of the resonance frequency, the term $\propto (d_\perp - d_\parallel)/R$ emerging in the pole of the polarizability [26, 34] [the generalized version of Eq. (14) for arbitrary ε_+ and ε_d] now acquires a finite contribution also from z_0, which may lead to a net blueshift of the dipolar LSP resonance. This behavior is also in line with recent experimental observations of the dependence of quantum size effects on the local dielectric environment of the interface [84] (notice that Eqs. (15) also enable further explorations of situations where $\varepsilon_d > 1$). As illustrated in Figure 3, the combined effects of a non-unity interband permittivity, ε_+, and of a finite z_0 may render the redshift of the classical dipolar LSP resonance frequency into a net blueshift, depending on both ε_+ and z_0/a (and also on the particular value of the bulk-damping parameter, γ, which "softens" the sharp feature at $\omega = \omega_p$; see Figure 2b). In this way, the model conceptually explains how different metals may exhibit contrasting $1/R$ size-dependencies of their surface plasmon resonances [22, 51, 85], towards the blue for $d_{eff} < 0$ (spill-in) and toward the red for $d_{eff} > 0$ (spill-out). An example of the former is silver (characterized by significant interband and valence band screening contributions to the optical response) [22, 36, 86], while an example of the latter is sodium (whose optical response is well described by a simple jellium treatment) [22]. The imaginary part $\mathrm{Im}\left(d_\perp - d_\parallel\right)$ is a source of nonclassical $1/R$ size-dependent broadening [26, 34]. To experimentally resolve nonclassical size-dependent shifts, it is naturally preferable that $|\mathrm{Re}\left(d_\perp - d_\parallel\right)| \gg \mathrm{Im}\left(d_\perp - d_\parallel\right)$, so that the spectral shift is not rendered unobservable due to damping.

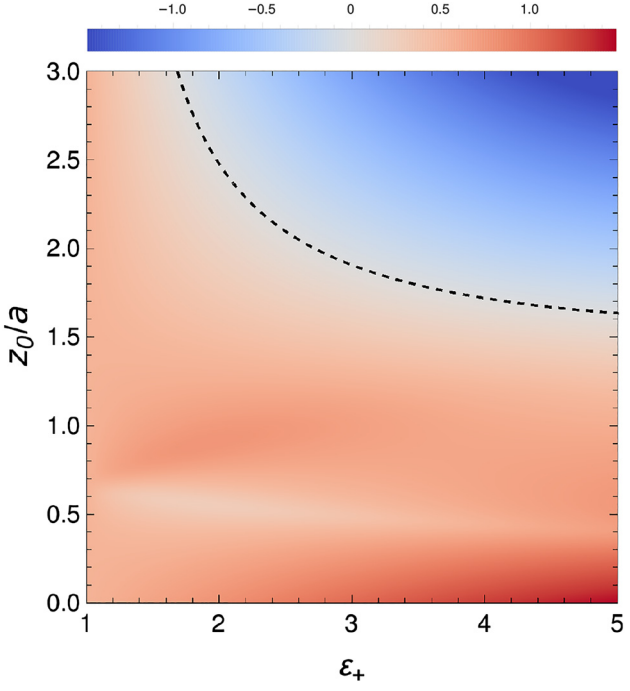

Figure 3: Density plot of $\mathrm{Re}\left(d_\perp - d_\parallel\right)/a$ in the (ε_+, z_0)-parameter space, computed at the classical quasistatic dipole LSP resonance frequency, $\omega = \omega_p/\sqrt{\varepsilon_+ + 2}$, of a spherical particle of radius R. The black dashed line indicates $\mathrm{Re}\left(d_\perp - d_\parallel\right) = 0$, thus separating regimes with nonclassical $1/R$ size-dependent spectral redshifts [reddish regions; $\mathrm{Re}\left(d_\perp - d_\parallel\right) > 0$] from blueshifts [bluish regions; $\mathrm{Re}\left(d_\perp - d_\parallel\right) < 0$]. We have assumed: $\varepsilon_d = 1$ and $\gamma/\omega_p = 0.1$.

3 Discussion and conclusions

In this article, we have revisited the concept of surface-response functions, highlighting that a finite contribution to the Feibelman d-parameters emerges even in an LRA-treatment with a spatially varying equilibrium electron-density profile. While this insight has appeared in some form within the early literature [59–62], it has seemingly remained unnoticed in the more recent revival of surface-response functions and the widespread use of *ab initio* accounts for quantum plasmonics. In working out the equilibrium contribution to the dynamic surface-response functions, we have deliberately omitted nonlocal corrections. In this context, the bulk nonlocal hydrodynamic response associated with the quantum compressibility of the electron gas would contribute with a negative $\mathrm{Re}\, d_\perp$ (well below the plasma frequency, and for a hard-wall jellium–vacuum interface), namely $d_\perp = -\beta/\left(\omega_p^2 - \omega^2\right)^{1/2}$ and $d_\parallel = 0$ [21, 26, 34, 40], with $\beta \propto v_F$ [5, 27, 87] being a characteristic velocity of longitudinal plasmons. Qualitatively, this could enhance regimes in Figure 3 with a net blueshift, while consequently also reducing the spectral shift in regimes with a net redshift. This possible interplay of quantum compressibility and quantum spill-out is manifested in self-consistent hydrodynamic treatments [13, 88, 89].

In conclusion, our analytical solution of the electrodynamics at metal surfaces transparently and unambiguously illustrates how the microscopic surface-response functions have a finite contribution originating entirely

from equilibrium and local-response considerations as input. We believe that this finding offers important insights for the understanding and further advancement of first-principle methods for the computation of accurate surface-response functions, as well as for the experimental exploration of mesoscopic optical phenomena at metal surfaces [35, 84, 86, 90, 91]. The latter is now becoming even more tangible with the advent of ultraconfined acoustic graphene plasmons [27, 31, 77, 92–94]. Beyond the fundamental interest in surface-response functions, we note that the underlying quantum nonlocal response of metals should also pose fundamental limitations for many light–matter interaction phenomena [95], ranging from plasmon-emitter interaction dynamics [26, 96, 97], through surface-enhanced Raman spectroscopy [98] and plasmon-exciton strong-coupling dynamics [99], to hyperbolic metamaterials [100], non-reciprocal plasmon propagation [101], and the perfect-lens concept [102] — the final example also illustrating the many insightful contributions by Mark Stockman.

Acknowledgement: This paper is dedicated to Mark I. Stockman in appreciation of his pioneering contributions to the broad area of Nano Optics. We thank T. Christensen for valuable discussions and P. M. Frederiksen for facilitating the writing of the manuscript.

Author contribution: All the authors have accepted responsibility for the entire content of this submitted manuscript and approved submission.

Research funding: N. A. M. is a VILLUM Investigator supported by VILLUM FONDEN (Grant No. 16498) and Independent Research Fund Denmark (Grant No. 7026-00117B). J. D. C. is a Sapere Aude research leader supported by Independent Research Fund Denmark (Grant No. 0165-00051B). C. W. acknowledges funding from a MULTIPLY fellowship under the Marie Skłodowska-Curie COFUND Action (grant agreement No. 713694). The Center for Nano Optics is financially supported by the University of Southern Denmark (SDU 2020 funding). The Center for Nanostructured Graphene is sponsored by the Danish National Research Foundation (Project No. DNRF103).

Conflict of interest statement: The authors declare no conflicts of interest regarding this article.

References

[1] J. D. Jackson, *Classical Electrodynamics*, New York, Wiley & Sons, 1998.

[2] A. Maradudin, J. R. Sambles, and W. L. Barnes, *Modern Plasmonics*, Amsterdam, North-Holland, 2014.

[3] G. Barton, "Some surface effects in the hydrodynamic model of metals," *Rep. Prog. Phys.*, vol. 42, no. 6, pp. 963–1016, 1979.

[4] J. M. Pitarke, V. M. Silkin, E. V. Chulkov, and P. M. Echenique, "Theory of surface plasmons and surface plasmon polaritons," *Rep. Prog. Phys.*, vol. 70, pp. 1–87, 2007.

[5] S. Raza, S. I. Bozhevolnyi, M. Wubs, and N. A. Mortensen, "Nonlocal optical response in metallic nanostructures," *J. Phys.: Condens. Matter*, vol. 27, p. 183204, 2015.

[6] M. I. Stockman, "Nanoplasmonics: past, present, and glimpse into future," *Opt. Express*, vol. 19, no. 22, pp. 22029–22106, 2011.

[7] A. I. Fernández-Domínguez, F. J. García-Vidal, and L. Martín-Moreno, "Unrelenting plasmons," *Nat. Photonics*, vol. 11, no. 1, pp. 8–10, 2017.

[8] O. Keller, M. Xiao, and S. I. Bozhevolnyi, "Optical diamagnetic polarizability of a mesoscopic metallic sphere: transverse self-field approach," *Opt. Commun.*, vol. 102, no. 3, pp. 238–244, 1993.

[9] Z. F. Öztürk, S. Xiao, M. Yan, M. Wubs, A.-P. Jauho, and N. A. Mortensen, "Field enhancement at metallic interfaces due to quantum confinement," *J. Nanophotonics*, vol. 5, no. 1, p. 051602, 2011.

[10] C. David and F. J. García de Abajo, "Surface plasmon dependence on the electron density profile at metal surfaces," *ACS Nano*, vol. 8, no. 9, pp. 9558–9566, 2014.

[11] F. J. García de Abajo, "Nonlocal effects in the plasmons of strongly interacting nanoparticles, dimers, and waveguides," *J. Phys. Chem. C*, vol. 112, no. 46, pp. 17983–17987, 2008.

[12] N. A. Mortensen, S. Raza, M. Wubs, T. Søndergaard, and S. I. Bozhevolnyi, "A generalized nonlocal optical response theory for plasmonic nanostructures," *Nat. Commun.*, vol. 5, p. 3809, 2014.

[13] G. Toscano, J. Straubel, A. Kwiatkowski, et al., "Resonance shifts and spill-out effects in self-consistent hydrodynamic nanoplasmonics," *Nat. Commun.*, vol. 6, p. 7132, 2015.

[14] A. Varas, P. García-González, J. Feist, F. J. García-Vidal, and A. Rubio, "Quantum plasmonics: from jellium models to *ab initio* calculations," *Nanophotonics*, vol. 5, no. 3, pp. 409–426, 2016.

[15] W. Zhu, R. Esteban, A. G. Borisov, et al., "Quantum mechanical effects in plasmonic structures with subnanometre gaps," *Nat. Commun.*, vol. 7, p. 11495, 2016.

[16] J. Zuloaga, E. Prodan, and P. Nordlander, "Quantum description of the plasmon resonances of a nanoparticle dimer," *Nano Lett.*, vol. 9, no. 2, pp. 887–891, 2009.

[17] J. Zuloaga, E. Prodan, and P. Nordlander, "Quantum plasmonics: optical properties and tunability of metallic nanorods," *ACS Nano*, vol. 4, no. 9, pp. 5269–5276, 2010.

[18] T. V. Teperik, P. Nordlander, J. Aizpurua, and A. G. Borisov, "Robust subnanometric plasmon ruler by rescaling of the nonlocal optical response," *Phys. Rev. Lett.*, vol. 110, no. 26, p. 263901, 2013.

[19] K. Andersen, K. L. Jensen, N. A. Mortensen, and K. S. Thygesen, "Visualizing hybridized quantum plasmons in

coupled nanowires: from classical to tunneling regime,'' *Phys. Rev. B*, vol. 87, no. 23, p. 235433, 2013.
[20] R. Sinha-Roy, P. García-González, H.-C. Weissker, F. Rabilloud, and A. I. Fernández-Domínguez, ''Classical and ab initio plasmonics meet at sub-nanometric noble metal rods,'' *ACS Photonics*, vol. 4, no. 6, pp. 1484–1493, 2017.
[21] P. J. Feibelman, ''Surface electromagnetic-fields,'' *Prog. Surf. Sci.*, vol. 12, no. 4, pp. 287–407, 1982.
[22] A. Liebsch, *Electronic Excitations at Metal Surfaces*, New York, Springer, 1997.
[23] H.-Y. Deng, ''A theory of electrodynamic response for bounded metals: surface capacitive effects,'' *Ann. Phys.*, vol. 418, p. 168204, 2020.
[24] S. I. Bozhevolnyi and N. A. Mortensen, ''Plasmonics for emerging quantum technologies,'' *Nanophotonics*, vol. 6, no. 5, p. 1185, 2017.
[25] A. I. Fernández-Domínguez, S. I. Bozhevolnyi, and N. A. Mortensen, ''Plasmon-enhanced generation of nonclassical light,'' *ACS Photonics*, vol. 5, no. 9, pp. 3447–3451, 2018.
[26] P. A. D. Gonçalves, T. Christensen, N. Rivera, A.-P. Jauho, N. A. Mortensen, and M. Soljačić, ''Plasmon–emitter interactions at the nanoscale,'' *Nat. Commun.*, vol. 11, p. 366, 2020.
[27] P. A. D. Gonçalves, *Plasmonics and Light–Matter Interactions in Two-Dimensional Materials and in Metal Nanostructures: Classical and Quantum Considerations*, Cham, Springer Nature, 2020.
[28] M. S. Tame, K. R. McEnery, Ş. K. Özdemir, J. Lee, S. A. Maier, and M. S. Kim, ''Quantum plasmonics,'' *Nat. Phys.*, vol. 9, no. 6, pp. 329–340, 2013.
[29] J. M. Fitzgerald, P. Narang, R. V. Craster, S. A. Maier, and V. Giannini, ''Quantum plasmonics,'' *Proc. IEEE*, vol. 104, no. 12, pp. 2307–2322, 2016.
[30] Z.-K. Zhou, J. Liu, Y. Bao, et al., ''Quantum plasmonics get applied,'' *Prog. Quant. Electron.*, vol. 65, pp. 1–20, 2019.
[31] P. A. D. Gonçalves, T. Christensen, N. M. R. Peres, et al., ''Quantum surface-response functions of metals revealed by acoustic graphene plasmons,'' *Nat. Commun.*, 2021, https://doi.org/10.1038/s41467-021-23061-8.
[32] P. Apell and D. R. Penn, ''Optical properties of small metal spheres: surface effects,'' *Phys. Rev. Lett.*, vol. 50, no. 17, pp. 1316–1319, 1983.
[33] W. Yan, M. Wubs, and N. A. Mortensen, ''Projected dipole model for quantum plasmonics,'' *Phys. Rev. Lett.*, vol. 115, no. 13, p. 137403, 2015.
[34] T. Christensen, W. Yan, A.-P. Jauho, M. Soljačić, and N. A. Mortensen, ''Quantum corrections in nanoplasmonics: shape, scale, and material,'' *Phys. Rev. Lett.*, vol. 118, no. 15, p. 157402, 2017.
[35] Y. Yang, D. Zhu, W. Yan, et al., ''A general theoretical and experimental framework for nanoscale electromagnetism,'' *Nature*, vol. 576, no. 7786, pp. 248–252, 2019.
[36] A. R. Echarri, P. A. D. Gonçalves, C. Tserkezis, F. J. García de Abajo, N. A. Mortensen, and J. D. Cox, ''Optical response of noble metal nanostructures: quantum surface effects in crystallographic facets,'' *Optica*, vol. 8, 2021. https://doi.org/10.1364/OPTICA.412122.
[37] D. Langreth and H. Suhl, *Many-Body Phenomena at Surfaces*, Orlando, Academic Press, 1984.
[38] P. J. Feibelman, ''Microscopic calculation of electromagnetic fields in refraction at a jellium-vacuum interface,'' *Phys. Rev. B*, vol. 12, no. 4, pp. 1319–1336, 1975.
[39] R. Carmina Monreal, T. J. Antosiewicz, and S. P. Apell, ''Diffuse surface scattering and quantum size effects in the surface plasmon resonances of low-carrier-density nanocrystals,'' *J. Phys. Chem. C*, vol. 120, no. 9, pp. 5074–5082, 2016.
[40] M. K. Svendsen, C. Wolff, A.-P. Jauho, N. A. Mortensen, and C. Tserkezis, ''Role of diffusive surface scattering in nonlocal plasmonics,'' *J. Phys.: Condens. Matter*, vol. 32, no. 39, p. 395702, 2020.
[41] O. Keller, ''Random-phase-approximation study of the response function describing optical second-harmonic generation from a metal selvedge,'' *Phys. Rev. B*, vol. 33, no. 2, pp. 990–1009, 1986.
[42] M. Ichikawa, ''Theory of localized plasmons for metal nanostructures in random-phase approximation,'' *J. Phys. Soc. Jpn.*, vol. 80, no. 4, p. 044606, 2011.
[43] M. Ichikawa, ''Theory of localized plasmons for metal nanostructures in dielectrics,'' *e-J. Surf. Sci. Nanotechnol.*, vol. 16, pp. 329–338, 2018.
[44] J. Friedel, ''The distribution of electrons round impurities in monovalent metals,'' *Philos. Mag. A*, vol. 43, no. 337, pp. 153–189, 1952.
[45] N. D. Lang and W. Kohn, ''Theory of metal surfaces: charge density and surface energy,'' *Phys. Rev. B*, vol. 1, no. 12, pp. 4555–4568, 1970.
[46] J. Lindhard, ''On the properties of a gas of charged particles,'' *Mat. Fys. Medd. K. Dan. Vidensk. Selsk.*, vol. 28, no. 8, pp. 1–57, 1954 [Online]. Available at: http://publ.royalacademy.dk/books/414/2859.
[47] N. D. Mermin, ''Lindhard dielectric function in the relaxation-time approximation,'' *Phys. Rev. B*, vol. 1, no. 5, pp. 2362–2363, 1970.
[48] B. Gallinet, J. Butet, and O. J. F. Martin, ''Numerical methods for nanophotonics: standard problems and future challenges,'' *Laser Photon. Rev.*, vol. 9, no. 6, pp. 577–603, 2015.
[49] J. Joannopoulos, S. Johnson, J. Winn, and R. Meade, *Photonic Crystals: Molding the Flow of Light*, 2nd ed. New Jersey, Princeton University Press, 2008.
[50] P. Dombi, Z. Pápa, J. Vogelsang, et al., ''Strong-field nano-optics,'' *Rev. Mod. Phys.*, vol. 92, no. 2, p. 025003, 2020.
[51] A. Liebsch, ''Dynamical screening at simple-metal surfaces,'' *Phys. Rev. B*, vol. 36, no. 14, pp. 7378–7388, 1987.
[52] P. Apell, ''A simple derivation of the surface contribution to the reflectivity of a metal, and its use in the van der Waals interaction,'' *Phys. Scripta*, vol. 24, no. 4, pp. 795–806, 1981.
[53] P. J. Feibelman, ''Interpretation of the linear coefficient of surface-plasmon dispersion,'' *Phys. Rev. B*, vol. 40, no. 5, pp. 2752–2756, 1989.
[54] D. Bedeaux and J. Vlieger, *Optical Properties of Surfaces*, London, Imperial College Press, 2004.
[55] F. Forstmann and R. R. Gerhardts, *Metal Optics Near the Plasma Frequency*, Berlin, Heidelberg, Springer-Verlag, 1986.

[56] D. C. Langreth, "Macroscopic approach to the theory of reflectivity," *Phys. Rev. B*, vol. 39, no. 14, pp. 10020–10027, 1989.
[57] F. Flores and F. García-Moliner, "Model-independent theory of surface plasmons," *Solid State Commun.*, vol. 11, no. 9, pp. 1295–1298, 1972.
[58] J. Harris and A. Griffin, "Surface plasmon dispersion," *Phys. Lett.*, vol. 34, no. 1, pp. 51–52, 1971.
[59] A. Bagchi, R. G. Barrera, and A. K. Rajagopal, "Perturbative approach to the calculation of the electric field near a metal surface," *Phys. Rev. B*, vol. 20, no. 12, pp. 4824–4838, 1979.
[60] P. J. Feibelman, "Interpretation of differential reflectance studies of metal surfaces," *Phys. Rev. B*, vol. 23, no. 6, pp. 2629–2634, 1981.
[61] P. Apell, "On the surface photoelectric effect in aluminum," *Phys. Scripta*, vol. 25, no. 1A, pp. 57–64, 1982.
[62] P. Apell, "Effects of non-locality and surface diffuseness on the electromagnetic response of a vacuum metal interface," *Solid State Commun.*, vol. 47, no. 8, pp. 619–622, 1983.
[63] A. Bagchi, "Transverse dielectric response of a semi-infinite metal: surface effect," *Phys. Rev. B*, vol. 15, no. 6, pp. 3060–3077, 1977.
[64] P. Ahlqvist and P. Apell, "On the hydrodynamical theory for surface plasmons," *Phys. Scripta*, vol. 25, no. 4, pp. 587–591, 1982.
[65] A. Bagchi, N. Kar, and R. G. Barrera, "Effect of refraction of *p*-polarized light on angle-resolved photoemission from surface states on metals," *Phys. Rev. Lett.*, vol. 40, no. 12, pp. 803–806, 1978.
[66] X. Liu, H. Kang, H. Yuan, et al., "Electrical tuning of a quantum plasmonic resonance," *Nat. Nanotechnol.*, vol. 12, no. 9, pp. 866–870, 2017.
[67] E. J. H. Skjølstrup, T. Søndergaard, and T. G. Pedersen, "Quantum spill-out in few-nanometer metal gaps: effect on gap plasmons and reflectance from ultrasharp groove arrays," *Phys. Rev. B*, vol. 97, no. 11, p. 115429, 2018.
[68] E. J. H. Skjølstrup, T. Søndergaard, and T. G. Pedersen, "Quantum spill-out in nanometer-thin gold slabs: effect on the plasmon mode index and the plasmonic absorption," *Phys. Rev. B*, vol. 99, no. 15, p. 155427, 2019.
[69] A. Taghizadeh and T. G. Pedersen, "Plasmons in ultra-thin gold slabs with quantum spill-out: Fourier modal method, perturbative approach, and analytical model," *Opt. Express*, vol. 27, no. 25, pp. 36941–36952, 2019.
[70] A. Rivacoba, "Electron spill-out effects in plasmon excitations by fast electrons," *Ultramicroscopy*, vol. 207, p. 112835, 2019.
[71] C. Henkel, G. Boedecker, and M. Wilkens, "Local fields in a soft matter bubble," *Appl. Phys. B*, vol. 93, pp. 217–221, 2008.
[72] J. M. Rogowska, K. F. Wojciechowski, and M. Maciejewski, "Analytical representation of the Lang–Kohn density profiles by the numerical fitting," *Acta Phys. Pol., A*, vol. 85, no. 3, pp. 593–601, 1994.
[73] T. Dethe, H. Gill, D. Green, et al., "Causality and dispersion relations," *Am. J. Phys.*, vol. 87, no. 4, pp. 279–290, 2019.
[74] B. N. J. Persson and P. Apell, "Sum rules for surface response functions with application to the van der Waals interaction between an atom and a metal," *Phys. Rev. B*, vol. 27, no. 10, pp. 6058–6065, 1983.
[75] B. N. J. Persson and E. Zaremba, "Electron-hole pair production at metal surfaces," *Phys. Rev. B*, vol. 31, no. 4, pp. 1863–1872, 1985.
[76] N. D. Lang and W. Kohn, "Theory of metal surfaces: induced surface charge and image potential," *Phys. Rev. B*, vol. 7, no. 8, pp. 3541–3550, 1973.
[77] P. A. D. Gonçalves, N. Stenger, J. D. Cox, N. A. Mortensen, and S. Xiao, "Strong light–matter interactions enabled by polaritons in atomically thin materials," *Adv. Opt. Mater.*, vol. 8, no. 5, p. 1901473, 2020.
[78] A. Reserbat-Plantey, I. Epstein, I. Torre, et al., "Quantum nanophotonics in two-dimensional materials," *ACS Photonics*, vol. 8, no. 1, pp. 85–101, 2021.
[79] T. Christensen, W. Yan, S. Raza, A.-P. Jauho, N. A. Mortensen, and M. Wubs, "Nonlocal response of metallic nanospheres probed by light, electrons, and atoms," *ACS Nano*, vol. 8, no. 2, pp. 1745–1758, 2014.
[80] F. Wang and Y. R. Shen, "General properties of local plasmons in metal nanostructures," *Phys. Rev. Lett.*, vol. 97, no. 20, p. 206806, 2006.
[81] P. Apell and Å. Ljungbert, "Red shift of surface plasmons in small metal particles," *Solid State Commun.*, vol. 44, no. 9, pp. 1367–1369, 1982.
[82] A. J. Bennett, "Influence of the electron charge distribution on surface-plasmon dispersion," *Phys. Rev. B*, vol. 1, no. 1, pp. 203–207, 1970.
[83] K.-D. Tsuei, E. W. Plummer, A. Liebsch, K. Kempa, and P. Bakshi, "Multipole plasmon modes at a metal surface," *Phys. Rev. Lett.*, vol. 64, no. 1, pp. 44–47, 1990.
[84] A. Campos, N. Troc, E. Cottancin, et al., "Plasmonic quantum size effects in silver nanoparticles are dominated by interfaces and local environments," *Nat. Phys.*, vol. 15, no. 3, pp. 275–280, 2019.
[85] A. Liebsch, "Surface-plasmon dispersion and size dependence of mie resonance: silver versus simple metals," *Phys. Rev. B*, vol. 48, no. 15, pp. 11317–11328, 1993.
[86] J. A. Scholl, A. L. Koh, and J. A. Dionne, "Quantum plasmon resonances of individual metallic nanoparticles," *Nature*, vol. 483, no. 7390, p. 421, 2012.
[87] P. Halevi, "Hydrodynamic model for the degenerate free-electron gas: generalization to arbitrary frequencies," *Phys. Rev. B*, vol. 51, no. 12, pp. 7497–7499, 1995.
[88] W. Yan, "Hydrodynamic theory for quantum plasmonics: linear-response dynamics of the inhomogeneous electron gas," *Phys. Rev. B*, vol. 91, no. 11, p. 115416, 2015.
[89] C. Ciracì and F. Della Sala, "Quantum hydrodynamic theory for plasmonics: impact of the electron density tail," *Phys. Rev. B*, vol. 93, no. 20, p. 205405, 2016.
[90] S. Raza, N. Stenger, S. Kadkhodazadeh, et al., "Blueshift of the surface plasmon resonance in silver nanoparticles studied with EELS," *Nanophotonics*, vol. 2, no. 2, pp. 131–138, 2013.
[91] S. Raza, S. Kadkhodazadeh, T. Christensen, et al., "Multipole plasmons and their disappearance in few-nanometer silver nanoparticles," *Nat. Commun.*, vol. 6, p. 8788, 2015.

[92] M. B. Lundeberg, Y. Gao, R. Asgari, et al., "Tuning quantum nonlocal effects in graphene plasmonics," *Science*, vol. 357, no. 6347, pp. 187–190, 2017.
[93] D. A. Iranzo, S. Nanot, E. J. C. Dias, et al., "Probing the ultimate plasmon confinement limits with a van der Waals heterostructure," *Science*, vol. 360, no. 6386, pp. 291–295, 2018.
[94] E. J. C. Dias, D. A. Iranzo, P. A. D. Gonçalves, et al., "Probing nonlocal effects in metals with graphene plasmons," *Phys. Rev. B*, vol. 97, no. 24, p. 245405, 2018.
[95] C. Ciracì, R. T. Hill, J. J. Mock, et al., "Probing the ultimate limits of plasmonic enhancement," *Science*, vol. 337, no. 6098, pp. 1072–1074, 2012.
[96] R. Filter, C. Bösel, G. Toscano, F. Lederer, and C. Rockstuhl, "Nonlocal effects: relevance for the spontaneous emission rates of quantum emitters coupled to plasmonic structures," *Opt. Lett.*, vol. 39, no. 21, pp. 6118–6121, 2014.
[97] C. Tserkezis, N. Stefanou, M. Wubs, and N. A. Mortensen, "Molecular fluorescence enhancement in plasmonic environments: exploring the role of nonlocal effects," *Nanoscale*, vol. 8, pp. 17532–17541, 2016.
[98] G. Toscano, S. Raza, S. Xiao, et al., "Surface-enhanced Raman spectroscopy: nonlocal limitations," *Opt. Lett.*, vol. 37, no. 13, pp. 2538–2540, 2012.
[99] C. Tserkezis, M. Wubs, and N. A. Mortensen, "Robustness of the Rabi splitting under nonlocal corrections in plexcitonics," *ACS Photonics*, vol. 5, no. 1, pp. 133–142, 2018.
[100] W. Yan, M. Wubs, and N. A. Mortensen, "Hyperbolic metamaterials: nonlocal response regularizes broadband supersingularity," *Phys. Rev. B*, vol. 86, no. 20, p. 205429, 2012.
[101] S. Buddhiraju, Y. Shi, A. Song, et al., "Absence of unidirectionally propagating surface plasmon-polaritons at nonreciprocal metal-dielectric interfaces," *Nat. Commun.*, vol. 11, p. 674, 2020.
[102] I. A. Larkin and M. I. Stockman, "Imperfect perfect lens," *Nano Lett.*, vol. 5, no. 2, pp. 339–343, 2005.

Supplementary Material: The online version of this article offers supplementary material (https://doi.org/10.1515/nanoph-2021-0084).